JACS
JOURNAL OF THE AMERICAN CHEMICAL SOCIETY
Article
pubs.acs.org/JACS

# Distance Dependent Electron Transfer at $TiO_2$ Interfaces Sensitized with Phenylene Ethynylene Bridged $Ru^{II}$–Isothiocyanate Compounds

Patrik G. Johansson,[†] Andrew Kopecky,[‡] Elena Galoppini,*[,‡] and Gerald J. Meyer*[,†]

[†]Departments of Chemistry and Materials Science & Engineering, Johns Hopkins University, 3400 North Charles Street, Baltimore, Maryland 21218, United States

[‡]Department of Chemistry, Rutgers University, 73 Warren St, Newark, New Jersey 07102, United States

Supporting Information

**ABSTRACT:** Excess electrons present in semiconductor nanocrystallites generate a significant electric field, yet the role this field plays in molecular charge transfer processes remains poorly understood. Three ruthenium bipyridyl *cis*-$Ru(bpy)(LL)(NCS)_2$ compounds, where LL is a 4-substituted bpy, with zero, one, or two phenylene ethynylene bridge units, were anchored to mesoporous nanocrystalline $TiO_2$ thin films to specifically quantify interfacial charge transfer with chromophores designed to be set at variable distances from the surface. Injection of electrons into $TiO_2$ resulted in a blue shift of the metal-to-ligand charge transfer absorption consistent with an underlying Stark effect. The electroabsorption data were used to quantify the electric field experienced by the compounds that decreased from 0.85 to 0.22 MV/cm as the number of OPE spacers increased from 0 to 2. Charge recombination on the $10^{-8}$–$10^{-5}$ s time scale correlated with the magnitude of the electric field with an apparent attenuation factor $\beta$ = 0.12 Å$^{-1}$. Slow components to charge recombination observed on the $10^{-4}$–$10^{-1}$ s time scale that were unaffected by temperature, irradiance, or the bridge units present on the molecular sensitizer were attributed to electron tunneling between $TiO_2$ acceptor states. The photocurrent efficiencies of solar cells based on these compounds decreased markedly when the bridge units were present on the sensitizer. Iodine was found to form adducts with all three compounds, $K = 1.8 \pm 0.2 \times 10^4$ M$^{-1}$, but only significantly lowered the excited state injection yield for those that possessed the bridge units.

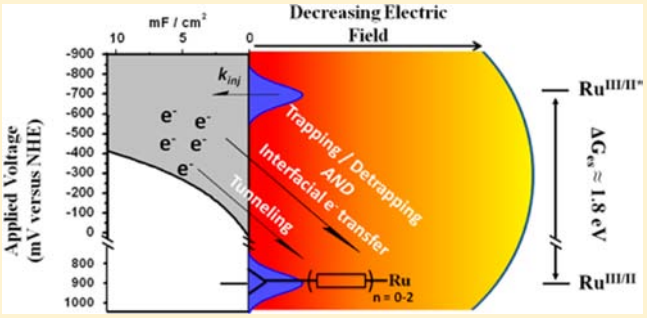


## INTRODUCTION

The fundamental behavior of metal-to-ligand charge-transfer (MLCT) excited states at conductive interfaces is relevant to applications in dye-sensitized solar cells (DSSCs) and organic light emitting diodes (OLEDs).[1−3] In DSSCs, ruthenium polypyridyl compounds, generically referred to as "sensitizers", anchored to nanocrystalline (anatase) $TiO_2$ have emerged as the most successful.[4,5] Under most conditions, the MLCT excited states are short-lived due to rapid electron transfer to the $TiO_2$ acceptor states, $S^*/TiO_2 \rightarrow S^+/TiO_2(e^-)$.[6−10] Indeed, electron injection on sub-picosecond time scales has been reported for many sensitized $TiO_2$ interfaces.[9,11] Under conditions where the energetics for excited state electron transfer are unfavorable, lateral intermolecular energy transfer across the semiconductor surface has been observed.[12,13] Since MLCT excited states are often long-lived, ultrafast injection is not necessarily required for high efficiency DSSCs. For many sensitizers, injection on nanosecond time scales would still be expected to occur with quantum yields near unity. A potential advantage of slower injection is that the rate constant for the unwanted charge recombination reaction between the oxidized sensitizer and the injected electron, $S^+/TiO_2(e^-) \rightarrow S/TiO_2$, may also be retarded. Slow recombination allows more time for hole transfer from the oxidized sensitizer to a redox mediator, behavior that is particularly important for sensitization to infrared light, where $S^+$ is a weak oxidant and the driving force for hole transfer is small.[14] Here we describe studies where charge recombination was inhibited by the presence of phenylene ethynylene, or what are sometimes called oligo-(phenylene ethynylene) (OPE), bridge units.

The introduction of a rigid bridge that controls the distance between the donor and acceptor is one approach by which electron transfer has been controlled in molecular compounds.[15−17] Quite often the influence of the bridge on the electron transfer rate constants is quantified through eq 1,

$$k_{et} = k_0 \exp(-\beta R_{DA}) \quad (1)$$

where $k_0$ is the rate constant at van der Waals separation, $R_{DA}$ is the donor–acceptor distance, and $\beta$ is the attenuation factor. The magnitude of $\beta$ has been correlated with the molecular details of the bridge in many literature reports.[15−17] At sensitized $TiO_2$ interfaces, distance dependencies are much less well understood in spite of many studies designed to

**Received:** March 1, 2013
**Published:** May 8, 2013

   dx.doi.org/10.1021/ja402193f | J. Am. Chem. Soc. 2013, 135, 8331−8341

quantify them.[18−28] Sensitizers with methylene bridges or rigid OPE and phenyl bridges positioned between the sensitizer and carboxylic acid surface binding groups have failed to provide consistent $\beta$ values. In a materials chemistry approach, core−shell structures comprising spherical $TiO_2$ cores coated with thin insulating metal oxide layers that electrons must tunnel through have been sensitized to visible light, but have also failed to show a systematic distance dependence for electron transfer.[22−24] Distance arguments have in fact been invoked to rationalize interfacial charge recombination trends where the "hole" was translated from the oxidized sensitizer to spatially isolated molecular orbitals on a pendant electron donor, but such behavior does not appear to be general.[25−28] In all these molecular−semiconductor interfaces, the true charge transfer distance remains speculative. Here we provide evidence that electroabsorption spectroscopy can be used as a direct *in situ* tool for the characterization of donor−acceptor distances at molecular−semiconductor interfaces.

Electron transfer in molecular donor−bridge−acceptor compounds is usually characterized when the concentration of oxidized donors and reduced acceptors are equal. At sensitizer−semiconductor interfaces, however, one is often most interested in situations where this is not the case. For example, in DSSCs under 1 sun illumination, the number of electrons in each $TiO_2$ nanocrystallite at the power point condition is about 20, while the steady state value for oxidized dyes is much less than 1.[5] The excess electrons have been quantified spectroscopically and by electrochemical means such as the charge extraction method.[1,5] These disparate concentrations of $TiO_2(e^-)$ and oxidized sensitizers may change the mechanism(s) of charge recombination from the second-order kinetics expected when the numbers are equal. Furthermore, the presence of excess electrons in $TiO_2$ generates an electric field that can influence redox potentials and electron transfer dynamics in a manner that is not well understood. This study reports the first example of interfacial charge recombination where the bridge and the number of $TiO_2(e^-)$s were systematically varied.

A previous letter reported $S^+/TiO_2(e^-) \rightarrow S/TiO_2$ charge recombination data for sensitizers **AK0** and **AK1** shown in Chart 1, under conditions where the number of injected electrons and oxidized sensitizers were equivalent.[29] The kinetic data were complex and modeled by a distribution of rate constants whose average value was larger for **AK0**/$TiO_2$. Here we take advantage of a recently discovered electro-absorption signature, similar to that observed in Stark spectroscopy,[30] and correlate electric field strength to charge recombination rate constants with the expanded series of sensitizers shown in Chart 1 where the distance from the Ru metal center to the anchoring oxygen atoms on the carboxylic acid groups are estimated to be 7, 12, and 18.6 Å. The data suggest that Stark spectroscopy can provide information on the magnitude of surface electric fields of molecular sensitizers positioned at variable distances from a semiconductor surface. The implications of these findings for solar energy conversion are discussed.

**Chart 1. The Ru(II)-Isothiocyanate Compounds Studied in This Work and Their Abbreviations**

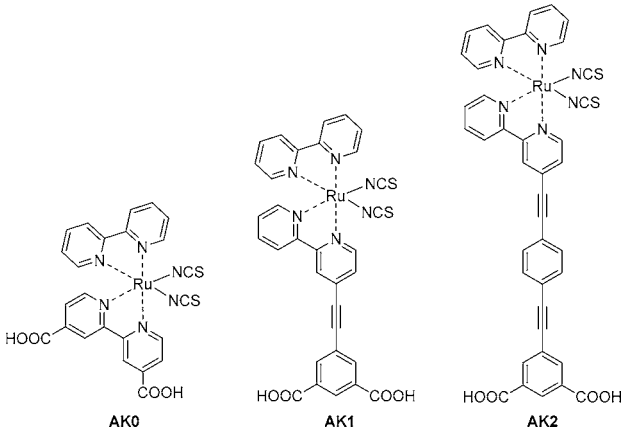


## EXPERIMENTAL SECTION

**Materials.** The following reagents and substrates were used as received, unless otherwise specified, from the indicated commercial suppliers: acetonitrile (Burdick& Jackson, spectrophotometric grade); toluene (OmniSolv, 99.99%); lithium perchlorate (Aldrich, 99.99%); *n*-tetrabutylammonium perchlorate (TBAP; Fluka, >99.9%); *n*-tetrabutylammonium chloride (TBACl; Sigma Aldrich, 98%); bis-(triphenylphosphine)palladium(II) chloride ($PdCl_2(PPh_3)_2$, Strem); triphenylphosphine palladium ($Pd(PPh_3)_4$, Strem); di-$\mu$-chlorobis[(*p*-cymene)chlororuthenium(II)] (Strem); *n*-tetrabutylammonium iodide (TBAI; Aldrich, >99% or Fluka, >98%); platinum(IV) chloride (Sigma Aldrich); silver nitrate (Bioanalytical Scientific Instruments, Inc.); hydrochloric acid (Fisher Scientific, 37.2% aqueous solution); argon gas (Airgas, >99.999%); oxygen gas (Airgas, industrial grade); dimethyl isophthalate (Sigma-Aldrich); *N*-bromosuccinimide (Sigma-Aldrich); tetra-*N*-butylammonium fluoride (Sigma-Aldrich); [(4-bromophenyl)ethynyl] (trimethyl)silane (Sigma-Aldrich); sodium nitrite (Sigma-Aldrich), potassium iodide (Sigma-Aldrich); ammonium thiocyanate (Sigma-Aldrich); copper(I)bromide (Sigma-Aldrich); titanium(IV) isopropoxide (Sigma-Aldrich, 97%); zirconium(IV) propoxide (Aldrich, 70 wt % solution in 1-propanol); $SnO_2$ colloidal solution (Alfa Aesar, 15% in water); anhydrous sodium sulfate ($Na_2SO_4$ VWR); *N*,*N*-dimethylformamide (VWR); 2,2′-dipyridyl (VWR); sodium hydroxide (NaOH, VWR); 10% Pd/C (Fisher-Acros); sodium bisulfate (Fisher-Acros); potassium dichromate (Fisher-Acros); tetra-N-butylammonium hydroxide (1.0 M in methanol, Alfa Aesar); fluorine-doped $SnO_2$-coated glass (FTO; Hartford Glass Co., Inc., 2.3 mm thick, 15 Ω/□); and microscope slides (Fisher Scientific, 1 mm thick); silica gel (230−400 mesh, Sorbent Technologies); hexanes (Pharmco) were distilled prior to use in column chromatography; diisopropyl amine (Pharmco) and dichloromethane (Pharmco) were distilled over calcium hydride; THF (Pharmco) was distilled with sodium and benzophenone; deuterated NMR solvents were purchased from Cambridge Isotopes.

**Sensitizer Synthesis.** The ruthenium isothiocyanate compounds **AK0−2** were prepared according to Scheme 1, adapting a tandem synthesis reported by Wang and co-workers for heteroleptic Ru complexes.[31] Compound **AK0** was prepared as a carboxylic acid by using the dcb ligand (2,2′-bipyridine-4,4′-dicarboxylic acid) in the first step. Ligands **5a** and **5b** were synthesized as previously reported.[32−36] Rigid-rod complexes **AK1** and **AK2** were prepared as esters, **6a** and **6b**, respectively to improve their solubility in inorganic solvents for the purification and characterization process, and were then hydrolyzed to acids. Compounds **AK1** and **AK2** were present as stereoisomeric mixtures since the isophthalic unit can be trans to the pyridyl unit or to the isothiocyanate ligand.

**General Procedure for the Synthesis of Complexes AK0, AK1, and AK2.**[31,37,38] Di-$\mu$-chlorobis[(*p*-cymene)chlororuthenium (**4**)] (1 equiv, 0.25−0.75 mmol) and the substituted dipyridyl ligand **5a**, **5b**, or **dcb** (2 equiv) were dissolved in DMF (160 mL/mmol of **4**) under $N_2$ and heated to 85 °C for 4 h, forming an orange-red solution. 2,2′-Dipyridyl (2 equiv) was added, and the reaction mixture was heated to 150 °C for an additional 4 h, upon which time the solution darkened. An excess of ammonium thiocyanate (15 equiv) was then added and the reaction mixture was maintained at 150 °C with stirring


dx.doi.org/10.1021/ja402193f | J. Am. Chem. Soc. 2013, 135, 8331−8341

**Scheme 1. Synthesis of Sensitizers AK0, AK1, and AK2**

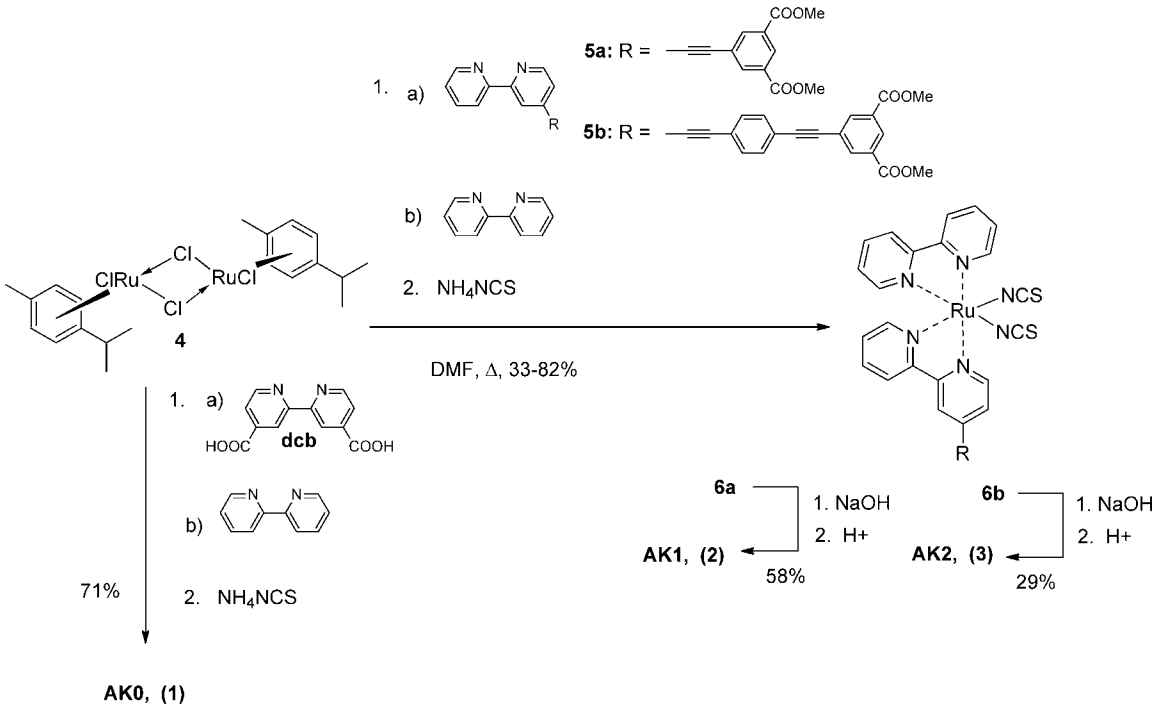


for an additional 4 h. The reaction mixture was allowed to cool to room temperature overnight and then the solvent was removed in vacuum. Water was added to the purple crude product, and the suspension was sonicated for 10 min. At this point, esters **6a** and **6b** were collected via vacuum filtration and washed with water. For carboxylic acid **1**, the pH of the suspension was adjusted to approximately pH 2 with 0.2 M $HNO_{3(aq.)}$. The suspension was refrigerated (5 °C) overnight, then filtered, the purple solid washed with water, and the precipitate was collected to afford **1**.

**Ru(NCS)$_2$[2,2′-Dipyridyl][2,2′-bipyridine-4,4′-dicarboxylic acid], AK0 (1).** The complex was prepared from **4** (303 mg, 0.496 mmol), 4,4′-dicarboxylic acid-2,2′-bipyridine (248 mg, 1.00 mmol), DMF (87 mL), 2,2′-dipyridyl (158 mg, 1.00 mmol), and ammonium thiocyanate (578 mg, 7.605 mmol) were used. Yield: 0.440 g, 71%. $^1$H NMR (DMSO): $\delta_H$ 9.43 (d, $J$ = 5.7, 1H), 9.27 (d, $J$ = 5.5, 1H), 9.07 (s, 1H), 8.91 (s, 1H), 8.77 (d, $J$ = 8.1, 1H), 8.62 (d, $J$ = 8.1, 1H), 8.28 (t, $J$ = 7.3, 2H), 7.97 (t, $J$ = 6.7, 1H), 7.91 (t, $J$ = 8.2, 1H), 7.76 (d, $J$ = 5.6, 1H), 7.61 (d, $J$ = 5.5, 1H), 7.52 (d, $J$ = 5.5, 1H), 7.29−7.18 (m, 1H). ESI$^+$: calculated, 640.9615 [M+Na]$^+$; found: 640.9793 [M+Na]$^+$.

**Methyl Ester 6a.** The complex was prepared from **4** (150 mg, 0.245 mmol), **5a** (182 mg, 0.489 mmol), DMF (43 mL), 2,2′-dipyridyl (78 mg, 0.489 mmol), and ammonium thiocyanate (250 mg, 3.2 mmol). Yield: 0.300 g, 82.12%. $^1$H NMR (DMSO): $\delta_H$ 9.33 (d, $J$ = 5.8), 9.29 (d, $J$ = 4.7), 9.02 (s), 8.87 (s), 8.85 (d, $J$ = 8.0), 8.79−8.73 (m), 8.71 (d, $J$ = 8.1), 8.65−8.58 (m), 8.54 (s), 8.48 (s), 8.46 (s), 8.33 (s), 8.30−8.19 (m), 8.10 (d, $J$ = 5.8), 7.99−7.91 (m), 7.91−7.84 (m), 7.67−7.62 (m), 7.59 (d, $J$ = 5.6), 7.57−7.51 (m), 7.37 (d, $J$ = 5.8), 7.32−7.22 (m), 3.95 (s), 3.91 (s). $^1$H NMR data shows an integration ratio of 17.5:6 for protons in the aromatic region to protons on the methyl ester, with the proton peak for the two stereoisomers occurring at 3.95 and 3.91 ppm. $^{13}$C NMR (DMSO): $\delta_C$ 164.54, 164.47, 162.27, 159.12, 158.35, 158.19, 158.13, 157.85, 157.63, 157.04, 156.96, 156.77, 156.56, 152.28, 151.53, 151.48, 136.77, 136.65, 136.49, 136.12, 136.02, 135.92, 135.77, 133.58, 133.39, 131.22, 131.11, 128.84, 128.02, 127.96, 127.29, 127.04, 126.92, 126.34, 126.33, 126.25, 125.36, 125.12, 123.79, 123.69, 123.52, 123.50, 123.43, 123.39, 123.35, 123.31, 122.50, 122.37, 93.49, 88.43, 87.98, 52.82 (2C, −methyl ester), 52.77 (2C′, −methyl ester). The presence of stereoisomers results in splitting of the 52.82 and 52.77 methyl ester. Due to the low solubility and the presence of stereoisomers, an accurate assignment of the NMR spectra is not possible. ESI$^+$: calculated, 769.0244 [M+Na]$^+$, 784.9983 [M+K]$^+$; found, 769.0328 [M+Na]$^+$, 785.0070 [M+K]$^+$.

**Methyl Ester 6b.** The complex was prepared from **7** (357 mg, 0.758 mmol), **4** (231 mg, 0.379 mmol), DMF (55 mL), 2,2′-dipyridyl (116 mg, 0.757 mmol), and ammonium thiocyanate (432 mg, 5.69 mmol). Yield: 0.225 g, 33.6%. $^1$H NMR (DMSO): $\delta_H$ 9.31 (d, $J$ = 5.9), 9.28 (dd, $J$ = 7.9, 5.7), 8.95 (s), 8.85 (d, $J$ = 8.4), 8.80−8.78 (m), 8.78−8.68 (m), 8.61 (dd, $J$ = 13.2, 6.0), 8.46 (d, $J$ = 9.8), 8.34 (d, $J$ = 1.2), 8.31 (d, $J$ = 1.2), 8.29−8.20 (m), 8.04 (dd, $J$ = 6.1, 1.0), 7.99−7.85 (m), 7.79 (s), 7.72 (d, $J$ = 8.3), 7.69−7.61 (m), 7.60−7.49 (m), 7.32 (dd, $J$ = 6.0, 1.1), 7.31−7.23 (m), 3.93 (s), 3.91 (s). The $^1$H NMR data shows an integration ratio of 22:6 for protons in the aromatic region to protons on the methyl ester, with the protons from the methyl ester appearing at 3.93 and 3.91 ppm for each stereoisomer. Due to the splitting of peaks, isomerization, and the low solubility, more accurate proton assignment was not possible. The $^{13}$C NMR spectrum was not recorded due to the low solubility. ESI$^+$: calculated, 869.0559 [M+Na]$^+$; found, 869.0550 [M+Na]$^+$.

**General Procedure for Hydrolysis of Esters to Acids.**[39] Methyl esters **6a** and **6b** were dissolved in freshly distilled dichloromethane (2500 mL/mmol complex), and 2 N solution of NaOH in methanol (250 mL/mmol complex) was added; and the mixture was stirred at room temperature for 4 days. Water was added, and the mixture was extracted with water. Approximately 0.5 M HCl was used to neutralize the aqueous solution to approximately pH 3 and precipitate the product. The product was then filtered, and DMF was used to recover the purple solid.

**AK1 (2): Methyl Ester 6a.** **6a** (23 mg, 0.031 mmol), freshly distilled dichloromethane (55 mL), and 2 N NaOH solution in methanol (7 mL) were used. Yield: 0.013 g, 58.5%. ESI+: calculated, 740.9930 [M+Na+], 756.9669 [M+K+]; found, 741.0118 [M+Na+], 756.9857 [M+K+].

**AK2 (3): Methyl Ester 6b.** **6b** (18 mg, 0.021 mmol), freshly distilled dichloromethane (50 mL), 2 N NaOH solution in methanol (6 mL) were used. Yield: 0.005 g, 29.3%. ESI$^+$: calculated, 841.0245 [M+Na]$^+$; found, 841.0250 [M+Na]$^+$.

**Sensitized Metal Oxide Thin Films.** Anatase $TiO_2$ nanocrystallites were prepared by hydrolysis of a Ti($i$-OPr)$_4$ precursor by a previously described sol−gel technique.[18] The sols were cast as mesoporous thin films (~10 $\mu$m thick) by doctor blading onto glass


dx.doi.org/10.1021/ja402193f | J. Am. Chem. Soc. 2013, 135, 8331−8341

**Table 1. Redox and Photoelectrochemical Properties of the Sensitized Thin Films**

| | $E_{1/2}(Ru^{III/II})$ (mV)[a] | | | | | | |
|---|---|---|---|---|---|---|---|
| sensitized film | $TiO_2$ | FTO | $E_{1/2}(Ru^{III/II*})$ (mV)[c] | $i$[d] | IPCE[e] | $\tau$[f] | $\phi_{inj}$[g] |
| AK0/$TiO_2$ | xx[b] | 940 | −660 | 1.85 ± 0.1 | 0.78 | 27 ± 5 | 0.98 ± 0.03 |
| AK1/$TiO_2$ | 900 | 930 | −700 | 3.20 ± 0.3 | 0.48 | 31 ± 5 | 0.93 ± 0.03 |
| AK2/$TiO_2$ | 880 | 910 | −730 | 3.40 ± 0.4 | 0.39 | 26 ± 5 | 0.70 ± 0.03 |

[a]The $Ru^{III/II}$ reduction potential measured for the indicated sensitizer anchored to fluorine-doped tin oxide (FTO) and $TiO_2$. [b]Irreversible redox chemistry was observed. [c]The excited state reduction potential. [d]Ideality factor (**i**). [e]Incident photon-to-current efficiency measured at 525 nm in 0.5 M LiI/0.05 M $I_2$. [f]Excited state lifetime at room temperature in $CH_3CN$. [g]Excited state injection yield quantified by comparative actinometry.

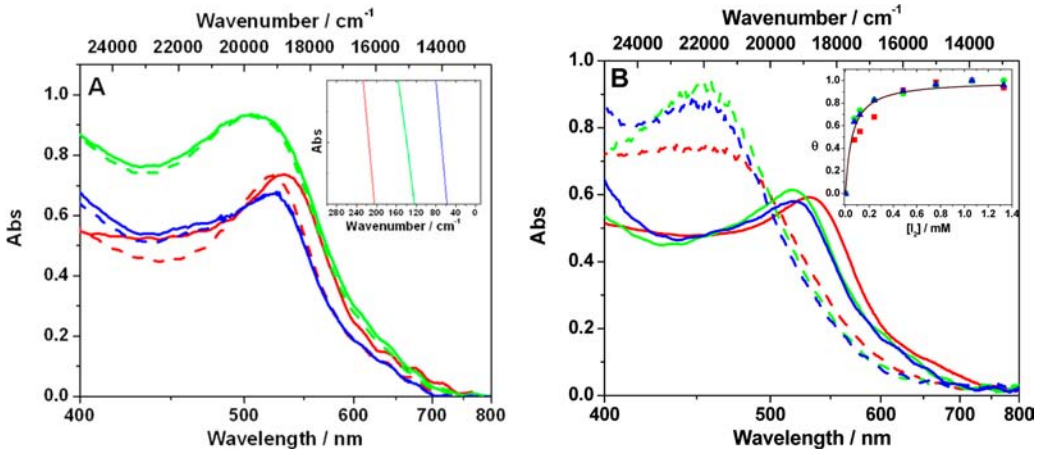


**Figure 1.** (A) Visible absorption spectra of **AK0**/$TiO_2$ (red), **AK1**/$TiO_2$ (green), and **AK2**/$TiO_2$ (blue) in 0.3 M $LiClO_4/CH_3CN$ with a bias of +300 mV (—) and −300 mV vs NHE (---). The inset shows the magnitude of the long wavelength absorption change measured from the data. (B) The visible absorption spectra of the sensitized thin films measured without (—) and with 1.03 mM $I_2$ (---). Inset show the fraction of $I_2$-adduct, $\theta$, as a function of the $I_2$ concentration with an overlaid fit to the Langmuir adsorption isotherm model, $K = 1.8 \pm 0.2 \times 10^4$ $M^{-1}$.

microscope slides for spectroscopic measurements and transparent conductive substrates (FTO) for electrochemical measurements. The thin films were annealed at 450 °C for 30 min under an atmosphere of $O_2$.

The sensitizers were anchored to the metal oxide film by reaction in a 0.5−2 mM solution of acetonitrile/*tert*-butanol (50/50 mixture, v:v). The sensitized metal oxide thin films were immersed in the solutions and then kept at 25 °C until the desired surface coverage was achieved. The cuvettes containing the thin film and electrolyte solution were purged with Ar(g) for at least 30 min prior to experimentation. The macroscopic surface coverage, Γ in mol/$cm^2$, was determined from the measured absorption with a modified Beer−Lambert law: Abs = 1000 × Γ × $\varepsilon$, where $\varepsilon$ was the molar decadic extinction (absorption) coefficient, $M^{-1}$ $cm^{-1}$, that was assumed to be the same in solution and on the surface. The saturation surface coverages were typically Γ ∼ 4.4 × $10^{-8}$ mol/$cm^2$ which corresponds to roughly 500 sensitizers per $TiO_2$ nanocrystallite.[5] Sensitized films were stored in acetonitrile for at least an hour before use.[19,20]

Counter electrodes were prepared by deposition of $PtCl_4$ dissolved in isopropanol onto FTO that was heated at 450 °C for 30 min under an atmosphere of $O_2$. The solar cell was completed by sandwiching the sensitized $TiO_2$ thin film and the Pt electrodes together with a 100 $\mu$m thick Surlyn film heated to ∼70 °C. An electrolyte solution of 0.5 M LiI and 0.05 M $I_2$ in acetonitrile was introduced between the electrodes through a hole drilled in the Pt-counter electrode. The hole was later sealed with Surlyn.

**Absorption Spectroscopy.** UV−vis absorbance spectra were collected using a Varian Cary 50 spectrometer or an Aviv spectrophotometer model 14NT-UV−vis at room temperature in a standard 1 cm path length quartz cuvette. Sensitized metal oxide slides were positioned at a 45° angle in a 0.3 M $LiClO_4/CH_3CN$ filled cuvette. The solutions were purged with argon gas for at least 30 min prior to absorption studies.

Nanosecond transient absorbance measurements were performed with a 532 nm laser excitation (ca. 8 ns fwhm at the magic angle) from a frequency doubled Nd:YAG Brilliant B Blue Sky. A pulsed 150 W Xe lamp coupled to a Spectral Energy GM-252 monochromator served as the probe light. The excitation fluency was measured with a thermopile power meter (Molectron). A Spex 1702/04 monochromator optically coupled to a 928 Hamamatsu photomultiplier tube with a computer interfaced LeCroy 9450 oscilloscope was employed for detection. Typically the absorption change measured after 60−100 laser pulses were averaged at each observation wavelength. For short time scales (<90 $\mu$s), the Xe lamp was pulsed and the sample was protected with a fast shutter, appropriate UV and heat absorbing glass, and solution filter combinations that also prevented PMT fatigue. The instrument response time was ∼10 ns.

In some experiments, an external bias was applied to the sensitized thin film in a spectroelectrochemical cell. In other experiments, the 514.5 nm line of an argon ion laser (Coherent) was used to illuminate the sensitized film. Comparative actinometry with $Ru^{II}(bpy)_3^{2+}$ and *cis*-$Ru^{II}(dcb)_2(NCS)_2/TiO_2$ was used to quantify the injection yields on nanosecond and longer time scales as previously described.[21,40] Low-temperature data were obtained with a liquid nitrogen CoolSpeK UV USP-203 four window cryostat (Unisoku).

**Photoluminescence.** Steady-state photoluminescence measurements were obtained with 514.5 nm excitation from an argon ion laser (Coherent Innova) and a double monochromator (SPEX 1682) optically coupled to a red sensitive Hamamatsu photomultiplier tube (Hamamatsu 636-10) for detection.

**Electrochemistry.** A potentiostat (BAS model CV-50W or Epsilon electrochemical analyzer) was employed for measurements in a standard three-electrode arrangement with a sensitized $TiO_2$ thin film deposited on an FTO substrate working electrode or a sensitized FTO slide working electrode,[41] a Pt gauze counter electrode, and a nonaqueous silver reference electrode (Bioanalytical Scientific Instruments, Inc.). The ferrocenium/ferrocene ($Fc^+$/Fc) half-wave potential measured in a 0.3 M $LiClO_4$ acetonitrile electrolyte was used as a standard to calibrate the reference electrode. Conversion to the normal

hydrogen electrode (NHE) was achieved with a conversion constant of −630 mV from NHE to $Fc^+/Fc$ in acetonitrile at 25 °C.[42]

**Photoelectrochemistry.** Photocurrent action spectra were measured in a two electrode configuration with a previously described apparatus that consisted of a PhotoMax 100 W Xe-lamp optically coupled to a 1/4 m Oriel Corner Stone monochromator.[43] Incident irradiances were measured with a calibrated silicon diode. Photocurrents were quantified with a Keithley 617 electrometer. The incident photon-to-current conversion efficiency (IPCE) was calculated as the number of injected electrons measured in the external circuit divided by the number of photons incident on the solar cell.

The open circuit photovoltages were measured as a function of incident 514.5 nm irradiance with an Ar ion laser. A two electrode configuration was employed with a sensitized $TiO_2$ thin film as the illuminated electrode and a Pt coated FTO electrode as the reference. Experiments with a Ag/AgCl reference electrode (Bioanalytical Scientific Instruments, Inc.) in 0.3 M $LiClO_4$ acetonitrile solution were conducted to ensure that the measured values were independent of the reference electrode. The voltage difference was measured with the Keithley electrometer before and after illumination. The incident irradiance was attenuated with neutral density filters.

## RESULTS

The three *cis*-Ru(bpy)(LL)$(NCS)_2$ coordination compounds shown in Chart 1 were synthesized and characterized spectroscopically. The visible absorption spectra of the compounds measured in fluid $CH_3CN$ were assigned to metal-to-ligand charge transfer (MLCT) transitions. Intense $\pi$-to-$\pi^*$ transitions were observed at 300 nm.[44] Both **AK1** and **AK2** displayed an additional absorption band in the 340−360 nm range that was assigned to the OPE bridge.[45] Light excitation into the MLCT absorption resulted in room temperature photoluminescence, PL. The PL maxima were 770 nm for **AK0** and **AK1**, and the maximum was 750 nm for **AK2**. Excited state relaxation was first-order with lifetimes of $\tau$ = 30 ± 4 ns, Table 1.

The compounds were anchored to nanocrystalline (anatase) $TiO_2$ thin films by immersing the films overnight in acetonitrile/*tert*-butanol solutions of the sensitziers. Typical surface coverages attained by this method were $4 \times 10^{-8}$ mol/cm$^2$. Shown in Figure 1A are representative absorption spectra of the sensitized thin films measured in a three electrode configuration with a +300 and a −300 mV applied bias. The spectra measured at +300 mV were within experimental error the same as that measured in the absence of an applied potential. With an applied bias of −300 mV, the characteristic absorption spectrum of reduced $TiO_2$, abbreviated $TiO_2(e^-)$, was observed and was subtracted from the data shown. The MLCT absorption was found to blue shift in the presence of $TiO_2(e^-)$.

To help visualize the MLCT absorption changes that accompanied $TiO_2$ reduction for all three sensitizers, the absorption shift in wavenumbers measured between 0.30 and 0.35 absorbance units are shown as the Figure 1 inset. A 190 cm$^{-1}$ change was observed for **AK0**/$TiO_2(e^-)$, and 100 and 40 cm$^{-1}$ change for **AK1**/$TiO_2(e^-)$ and **AK2**/$TiO_2(e^-)$, respectively. These spectral shifts were reversible when the $TiO_2(e^-)$ were removed from $TiO_2$ with a positive bias of +300 mV. Cathodic excursions negative of −350 mV resulted in absorption changes that were irreversible and were therefore avoided. Spectra that include contributions from $TiO_2(e^-)$ as well as unsensitized $TiO_2$ thin films are given in Figure S1 in the Supporting Information. The ATR-FTIR spectra for the sensitized thin films measured at open circuit revealed a broad band centered at 1630 cm$^{-1}$ assigned to the asymmetric $\nu_{co}$ stretch.

The absorption attributed to $TiO_2(e^-)$ increased exponentially with an applied negative bias, behavior consistent with many previous studies.[46] The absorption data were converted to a chemical capacitance using Faraday's Law, the electrode area, and the measured extinction coefficient of 1000 M$^{-1}$ cm$^{-1}$ at 800 nm, as was previously described.[46] We note that while this extinction coefficient is in good agreement with previous measurements,[1] it differs from a value recently reported for related materials.[47] The use of an alternative extinction coefficient would quantitatively change the magnitude of the capacitance, but would otherwise have no impact on the results of this paper that is largely comparative in nature. The capacitance as a function of applied potential is shown in Figure S1, with an overlaid fit to eq 2,

$$C = C_0 \exp\left(\frac{e}{ak_BT}V\right) \tag{2}$$

where $C$ is the measured chemical capacitance, $C_0$ is the capacitance intrinsic to the materials, that is, the total distribution of states that can store charge,[48] $T$ is the absolute temperature, and $k_B$ is the Boltzmann constant. The best fit gave $\alpha \approx 6$, a value that was within experimental error the same for sensitized and unsensitized thin films. An $\alpha = 6$ value was extracted from data measured on an unsensitized $TiO_2$ thin film that enabled characterization over a wider potential range.

The influence of 0 to 1.33 mM $I_2$ on the absorption spectra of the sensitized thin films was quantified in 0.3 M $LiClO_4$/$CH_3CN$, Figure 1B. The addition of $I_2$ to the external solution surrounding the films resulted in a significant blue shift in the MLCT absorption with the maintenance of an isosbestic point near 500 nm. Concentrations of $I_2$ greater than 1.33 mM had no further influence on the MLCT absorption. Shown in Figure 1B are the MLCT absorption spectra measured at 0 and 1.33 mM $I_2$ concentrations after contributions from $I_2$ were subtracted. The inset shows a Langmuir adsorption isotherm for the spectral changes observed at 450 nm with a best fit to eq 3,

$$\theta = \frac{K[I_2]}{1 + K[I_2]} \tag{3}$$

where $\theta$ is the fraction of sensitizer present in the $I_2$-adduct form.[49] The adduct formation constant, $K$, was estimated to be 1.8 ± 0.2 × 10$^4$ M$^{-1}$ for all three sensitizers. The spectral changes were found to be >90% reversible when $CH_3CN$ or iodide were added to the external solution.

Cyclic voltammograms of the sensitizers anchored to $TiO_2$ or to fluorine doped tin oxide (FTO) are shown in Supporting Information Figures S2 and S3. The electrochemistry measured on FTO was reversible as the cathodic and anodic currents were equal, $i_{pa}/i_{pc} = 1$, and the peak-to-peak separation $\Delta E_{pp}$ < 59 mV at a scan rate of 100 mV/s. The formal reduction potential for the three sensitized coordination compounds were as follows: **AK0**$^{III/II}$ = 950 mV, **AK1**$^{III/II}$ = 940 mV, and **AK2**$^{III/II}$ = 900 mV vs NHE. On $TiO_2$, the electrochemistry was irreversible for **AK0**/$TiO_2$ and quasi-reversible for the other two sensitizers with $i_{pa}/i_{pc} = 1$, and $\Delta E_{pp}$ > 100 mV. The excited state reduction potentials $E^0(Ru^{III/II*})$ were calculated with eq 4,

$$E^0(Ru^{III/II*}) = E^0(Ru^{III/II}) - \Delta G_{ES} \tag{4}$$


dx.doi.org/10.1021/ja402193f | J. Am. Chem. Soc. 2013, 135, 8331−8341

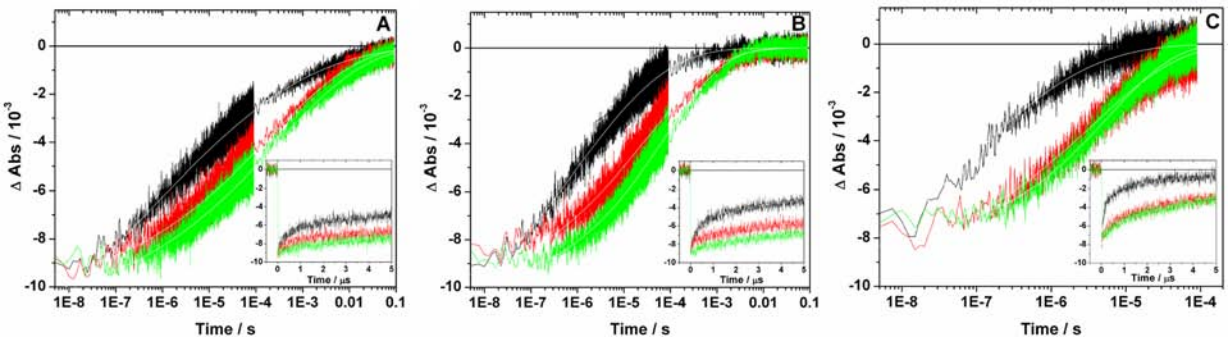


**Figure 2.** Transient absorption data monitored at 500 nm after pulsed 532 nm laser excitation (0.2 mJ/pulse) of **AK0**/$TiO_2$ (black), **AK1**/$TiO_2$ (red), and **AK2**/$TiO_2$ (green) in 0.3 M $LiClO_4$ $CH_3CN$ with an applied bias of (A) +150 mV, (B) −150 mV, and (C) −350 mV versus NHE. Overlaid are fits to a KWW kinetic model (white).

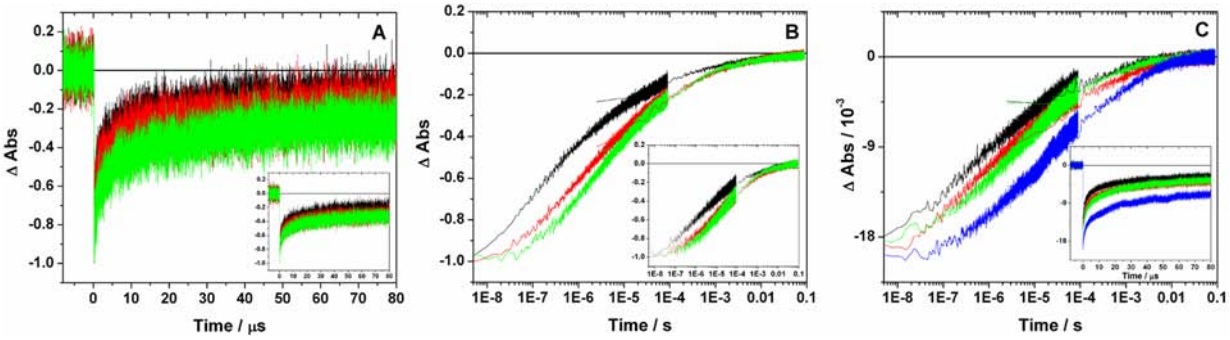


**Figure 3.** Transient absorption data monitored at 500 nm after pulsed 532 nm laser excitation (0.2 mJ/cm$^2$) of **AK0**/$TiO_2$ (black), **AK1**/$TiO_2$ (red), and **AK2**/$TiO_2$ (green) in 0.3 M $LiClO_4$/$CH_3CN$ under (A) steady state illumination (180 mW/cm$^2$ of 514.5 nm light); the inset shows without steady state illumination; (B) pulsed 1.4 mJ/cm$^2$ excitation irradiance while the inset shows 0.2 mJ/cm$^2$. The data in panel (C) was measured after pulsed laser excitation (1.0 mJ/cm$^2$) of **AK0**/$TiO_2$ at +40 °C (black), **AK0**/$TiO_2$ at −20 °C (red), **AK1**/$TiO_2$ at +40 °C (green), and **AK1**/$TiO_2$ at −20 °C (blue). The inset shows the first 80 $\mu$s.

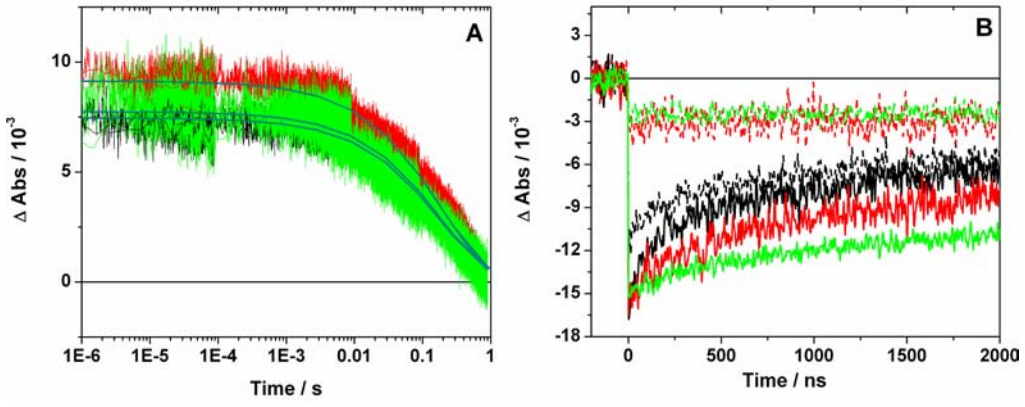


**Figure 4.** (A) Transient absorbance monitored at 375 nm after pulsed 532 nm excitation of **AK0**/$TiO_2$ (black), **AK1**/$TiO_2$ (red), and **AK2**/$TiO_2$ (green) in 0.5 M LiI/$CH_3CN$. Overlaid are solid line fits to the Kohlrausch−Williams−Watts model. (B) Transient absorbance monitored at 500 nm after pulsed 532 nm excitation of **AK0**/$TiO_2$ (black), **AK1**/$TiO_2$ (red), and **AK2**/$TiO_2$ (green) in 0.3 M $LiClO_4$/$CH_3CN$ in the absence (—) and presence (---) of 0.11 mM $I_2$.

where $\Delta G_{ES}$ is the free energy stored in the MLCT excited state. A tangent line on the high energy side of the corrected PL spectra, measured in solution, was used to obtain $\Delta G_{ES}$. The electrochemical data is summarized in Table 1.

Nanosecond transient absorption data were measured after pulsed laser excitation of the samples as the applied potential was varied from +350 to −350 mV vs. NHE. Transient data monitored at 500 nm with +150, −150, and −350 mV applied bias are shown in Figure 2 on a log time scale. The insets of Figure 2 show the first 5 $\mu$s of the same data plotted on a linear time scale. The ground state absorption and incident irradiance at 532 nm were the same for this study. Data recorded at other applied potentials are given in Figure S4 and Videos S1 and S2 in the Supporting Information. Overlaid on the data are best fits to the Kohlrausch−Williams−Watts (KWW) kinetic model, eq 5.

$$\mathrm{Abs}(t) = A_0 \exp[-(t/\tau_0)^{\beta'}] \quad (5)$$


dx.doi.org/10.1021/ja402193f | J. Am. Chem. Soc. 2013, 135, 8331−8341

Here $A_0$ is the initial absorption change, $\beta'$ is inversely related to the width of the underlying Lévy distribution of rate constants, $0 < \beta' < 1$, and $\tau_0$ is a characteristic lifetime.[50] Note that the data measured with a −350 mV applied bias is shown on a shorter time scale as recombination was much faster under these conditions.

The influence of steady state illumination on charge recombination was investigated with an argon ion laser ($\lambda$ = 514.5 nm, irradiance =180 mW/cm$^2$). This steady state irradiance increased the open circuit photovoltage by ∼200 mV relative to that measured with only the white light probe beam of the transient absorption apparatus. The spectral features observed after pulsed laser excitation were the same as that measured without steady state illumination, but the kinetics differed. This is shown by the comparison of Figure 3A and the inset. Significant increases in the charge recombination rate with the steady state irradiance were observed for **AK0**/$TiO_2$, while **AK1**/$TiO_2$ showed a very small increase with no measurable change for **AK2**/$TiO_2$.

The influence of pulsed 532 nm excitation fluency on charge recombination was also quantified at the open circuit condition. Figure 3B shows data measured with 1.4 mJ/pulse (for a 1 cm$^2$ area) and the inset show the same samples with an excitation fluency of 0.2 mJ/pulse. The higher fluency enhanced recombination at short time scales, but had no measurable influence on the long time scale data, see Supporting Information Video S3. Transient absorption data for the sensitized thin films was quantified from +40 to −20 °C, Figure 3C. The short time scale data was temperature dependent with no or very little dependence on the long time scale.

Transient absorption changes monitored at 375 nm after pulsed 532 nm excitation of the sensitized thin films immersed in 0.5 M LiI/$CH_3CN$ are shown in Figure 4A. Note that the data acquired on the sub 100 $\mu$s time were smoothed with a 20 data point average. The kinetic data was well described by the KWW model with $\beta$ = 0.61 and $k$ = 5.26 s$^{-1}$ for all three sensitized materials. The experiment was also performed with 0.63 mM $I_2$ in place of the 0.5 M LiI, Figure 4B. The initial amplitude of the absorption change was attenuated by about a factor of 6 for **AK1**/$TiO_2$ and **AK2**/$TiO_2$ yet had a much smaller ∼20% effect on **AK0**/$TiO_2$. In addition, kinetic data were also collected at 400 and 700 nm, where $I_2^{\bullet-}/I_3^-$ and $I_2^{\bullet-}$/$TiO_2(e^-)$ absorb light, respectively.[51] The presence of $I_2$ was found to lower the excited state injection yield without the formation of new chemical products.

The incident photon-to-current efficiency (IPCE) for the sensitized thin films were measured in 0.5 M LiI and 0.05 M $I_2$/$CH_3CN$, Supporting Information Figure S6A. With 525 nm excitation, the IPCE values were as follows: **AK0**/$TiO_2$ = 0.78, **AK1**/$TiO_2$ = 0.48, and **AK2**/$TiO_2$ = 0.39, Table 1. The open circuit voltage ($V_{oc}$) was measured in the absence of redox mediator in 0.3 M $LiClO_4$/$CH_3CN$ versus a reference electrode. Plots of $V_{oc}$ versus the log of the irradiance were linear with slopes of $i$ = 2, 3.2, and 3.4 for **AK0**/$TiO_2$, **AK1**/$TiO_2$, and **AK2**/$TiO_2$, respectively. This data is given in Supporting Information Figure S6B and summarized in Table 1.

## DISCUSSION

The goal of this work was to elucidate whether the kinetic rate constant for interfacial charge recombination, $k_{cr}$, was influenced by the surface electric field when the oxidized ruthenium compound was set at a variable distance from the $TiO_2$ surface. The sensitized interfaces were thus conceived with the hope that the interfacial energetics would be unchanged as the number of phenylene ethynylene bridge units was increased. This was found to approximately be the case. The $Ru^{III/II}$ reduction potentials varied by only 30 mV and the $TiO_2$ acceptor states were independent of the identity of the molecular sensitizer. Similar to the prototypical "N3" sensitizer,[52] that is, *cis*-Ru(dcb)$_2$(NCS)$_2$, the excited states characterized herein are potent reductants with favorable overlap with the $TiO_2$ acceptor states for efficient excited state injection, Figure 5.

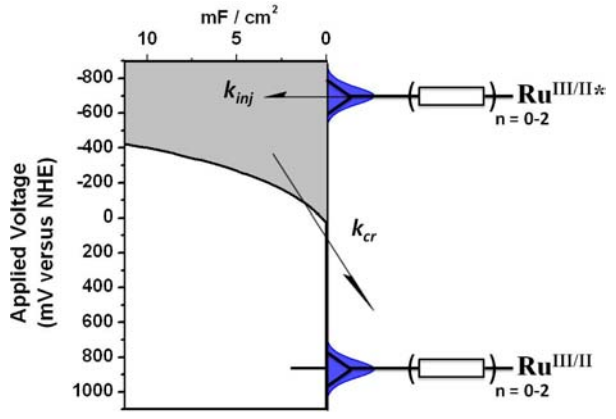


**Figure 5.** Energetics for excited state injection and charge recombination at the sensitized $TiO_2$ interfaces under study.

Furthermore, Stark spectroscopic data suggested that the *cis*-Ru(NCS)$_2$(bpy) core was on average further from the $TiO_2$ surface when phenylene ethynylene spacer were present between the bipyridyl ligand and the surface anchoring carboxylic acid groups. The magnitude of the electric field abstracted from such data was correlated with the $S^+/TiO_2(e^-) \rightarrow S/TiO_2$ charge recombination rate constants with a bridge length dependence indicating that the oxidized metal center was also further from the surface. The photophysical data measured in inert electrolytes indicated that sensitizers with phenylene ethynylene bridges would yield high efficiencies when utilized in a dye sensitized solar cell, yet this expectation was not realized and an unwanted quenching pathway with molecular iodine was identified. These behaviors are detailed below in the broader context of the relevant literature.

**I. Stark Effects.** The visible absorption spectra of the Ru(II) compounds are characteristic of metal-to-ligand charge-transfer (MLCT) transitions in ruthenium polypyridyl compounds. The spectra were specifically in agreement with expectations for *cis*-Ru(NCS)$_2$ polypyridyl compounds that display significant solar light harvesting through the visible region to about 700 nm.[1] Reflectance infrared studies show that the sensitizers bind to $TiO_2$ in their carboxylate form.[53]

The photoinduced or thermal transfer of electrons to $TiO_2$ is known to induce a blue shift of the MLCT absorption consistent with an underlying electric field, referred to as a Stark effect.[54] Here we found that the magnitude of the shift was largest for the sensitizer without a phenylene ethynylene bridge and smallest for that with two bridge units. When measured as an absorption difference with and without the presence of $TiO_2(e^-)$, the spectral data were well modeled by a first-derivative of the ground state absorption spectrum, consistent with an antiparallel alignment of the surface electric


dx.doi.org/10.1021/ja402193f | J. Am. Chem. Soc. 2013, 135, 8331−8341

field with the change in the sensitizer dipole moment vector, $\theta = 180°$. The magnitude of the spectral shift was directly related to the field strength through the change in the dipole moment, eq 6.[55]

$$\Delta\bar{\nu} = -\frac{|\Delta\vec{\mu}||\vec{E}|\cos\theta}{100hc} \quad (6)$$

The change in dipole moment for these compounds is unknown, however a value for *cis*-$Ru(dcb)_2(NCS)_2$ of $|\Delta\vec{\mu}| = 13.3$ D was reported.[56] Since the compounds under study all have a *cis* arrangement of the isothiocyanate ligands and the MLCT absorption is predominantly a Ru → bpy′ localized transition, we assert that this value represents a reasonable approximation for all three compounds. With this assumption, electric fields of magnitude $E = 0.85$, 0.45, and 0.20 MV/cm were calculated for these sensitized materials as the number of OPE units was increased from zero to two. While some surface heterogeneity and the presence of necking regions between the $TiO_2$ nanocrystallites within the mesoporous thin film are expected, the data indicates that the "average" field strength experienced by the chromophoric portion of the sensitizers is that expected when the sensitizers are oriented normal to the $TiO_2$ surface. Abstraction of a true distance between the *cis*-$Ru(NCS)_2$(bpy)-core and the $TiO_2$ interface was complicated by the aforementioned heterogeneity, the unknown location of the trapped electrons, and the unknown interfacial dielectric constant. Nevertheless, the Stark data support the notion that on average **AK2** was further from the $TiO_2$ surface then was **AK1** than **AK0**.

The significant electroabsorption measured for **AK0**/$TiO_2(e^-)$ that decreased in magnitude by about 1/2 and 1/4 as the phenylene ethynylene bridge units were incorporated are reminiscent of previous redox titrations reported by Gregg, Zaban, and Ferrere.[57] These investigators found that the reduction potentials of molecules located within the electric double layer were profoundly influenced by surface electric fields, while molecules outside were far less sensitive.[57] This raises the question of what the actual $E^0(Ru^{III/II})$ reduction potentials are when electrons are injected into $TiO_2$ and the electric field is large. The persistence of such large electric fields indicates that the anatase $TiO_2$ and the acetonitrile electrolyte do not quantitatively screen the field. A small distance between the $TiO_2(e^-)$ and the sensitizer would inhibit substantial screening by the electrolyte while the bridge units enable more substantial screening. Indeed the notion that **AK0** is within the inner Helmholtz layer while **AK1** and **AK2** are outside the double layer represents a simplified model in which much of the electron transfer dynamics described below can be understood.

**II. Interfacial Electron Transfer.** Recombination of an injected electron with an oxidized sensitizer represents an unwanted reaction that wastes energy and yields ground state products. This reaction has previously been studied by several research groups, mainly by time-resolved absorption spectroscopy.[1,2] The results described herein provide new insights into this important reaction. Comparative experiments were performed where the number of absorbed photons, the applied potential (and hence the $TiO_2(e^-)$ concentration), and the temperature were controlled. In discussions of these results, it is convenient to consider two separate time scales of charge recombination: *slow* (i.e., $10^{-4}$–$10^{-1}$ s) reactions and *fast* (i.e., $10^{-7}$–$10^{-4}$ s) reactions.

The *slow* charge recombination kinetics processes were insensitive to the identity of the molecular sensitizer, the temperature, and the incident irradiance. The data suggest a temperature independent rate limiting electron tunneling step as was proposed by Furube and Katoh.[58] It was curious that this slower tunneling process was insensitive to the number of bridge units, given that the faster recombination processes were (see below). A mechanism where electron tunneling between acceptor states rate limits a more rapid electron transfer to the oxidized sensitizer was therefore most consistent with this data.

The *fast* charge recombination dynamics were found to be sensitizer dependent, behavior that was most pronounced when the steady state illumination, $TiO_2(e^-)$ concentration, and/or the pulsed laser fluence were increased. Potentiostatic control of the sensitized thin film was employed to increase the concentration of $TiO_2(e^-)$s, a mechanistic approach first reported by O′Regan and co-workers,[59] that was later effectively utilized by the Durrant group[60] who found that an increased $TiO_2(e^-)$ concentration resulted in enhanced charge recombination rates. Here we find similar behavior with the extent of the enhancement being directly related to the number of bridge units present in the sensitizer.

When the $TiO_2(e^-)$ concentration was high, the *slow* components for charge recombination were not observed, presumably because the redox active states responsible for them were filled and tunneling between them was therefore absent. Under such conditions, the use of the KWW function, which is a paradigm for modeling transport in disordered materials like these $TiO_2$ thin films,[61] was of questionable value even though it did accurately model the experimental data. We therefore utilized a simple $t_{1/2}$ analysis or considered the fraction of charge recombination that occurred under specific conditions. With low irradiances and at open circuit or with a forward bias of +200 mV, change recombination over the first 85 μs was negligible for all the sensitized materials under study. As the quasi-Fermi level of the $TiO_2$ nanocrystallites was raised to +50 mV, about 20% of the electrons injected from **AK0**/$TiO_2$ had recombined while there was no measurable change for **AK1** or **AK2**. A forward bias of −50 and −150 mV were required to promote the same 20% increase in charge recombination for **AK1** and **AK2**, Figure 6. Stark spectroscopy showed that the field generated by $TiO_2(e^-)$s was strongly felt by **AK0**, but to a much lesser extent by **AK1** and **AK2**. Taken together, these

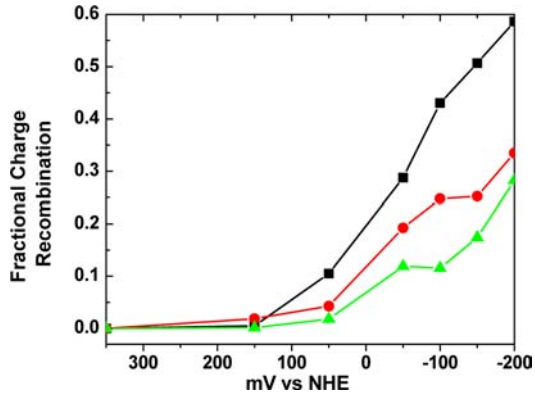


**Figure 6.** Fraction of charge recombination that occurred over the first 85 μs after pulsed 532 nm laser excitation as a function of the applied bias (black square, **AK0**/$TiO_2$), (red circle, **AK1**/$TiO_2$), and (green up-triangle, **AK2**/$TiO_2$).


dx.doi.org/10.1021/ja402193f | J. Am. Chem. Soc. 2013, 135, 8331−8341

data indicate that charge recombination can be inhibited with distance particularly when the number of injected electrons is large. These conditions are relevant to the power point of operational solar cells where over 20 electrons are expected to reside in each $TiO_2$ nanocrystallite as well as the open circuit condition where the number is even larger.[5] Such behavior is particularly evident with videos provided in the Supporting Information, and this almost certainly contributes to the unusually high irradiance dependence of the open circuit photovoltage, $V_{oc}$, measured with ideality factors greater than 3.[29]

Previous time-of-flight and intensity-modulated photocurrent measurements have shown that the apparent diffusion constant for charge transport through the $TiO_2$ thin films increased with the number of $TiO_2(e^-)$s, behavior that has been rationalized with trap filling models.[62−64] Such transport also involves the movement of ions, such as $Li^+$, and is often termed *ambipolar diffusion*. It is thus postulated that the observed rate constants abstracted from data measured under forward bias represent and hence high $TiO_2(e^-)$ concentrations most accurately reflect the true interfacial electron transfer rate constants for charge recombination. The transient data measured at −350 mV were thus fit to a distributional model based on a Levy distribution of rate constants, or simply to the time required for half of the charge separated states to recombine, $t_{1/2}$. The latter analysis revealed a significant distance dependence with an attenuation factor of $\beta \sim 0.12$ Å$^{-1}$. Note that the sensitizer AK0 was not included in this analysis as it did not contain a bridge unit and hence was not homologous with the other two sensitizers. While this value was abstracted from only the two bridged sensitizers and is subject to a rather large uncertainty, previously published data indicate that the mesoporous nature of the $TiO_2$ thin films likely preclude analysis over larger distances.[65]

The notion that the short time scale data measured at open circuit reports predominantly on charge recombination to the oxidized sensitizer while the slower time scale data reports on the electron tunneling between acceptor states is consistent with most previous literature reports at sensitized $TiO_2$ interfaces,[1,5] and helps rationalize why some investigators have found that charge recombination was highly sensitive to the thermodynamic driving force[66] while others found recombination to be essentially independent of driving force.[24,67] High injection fluxes and a low density of acceptor states with short observation times reflect conditions relevant to interfacial electron transfer while low injection fluxes, high acceptor densities, and long observation times reflect electron tunneling between acceptor states.

**III. Light-to-Electrical Energy Conversion.** Rapid excited state injection with slow microsecond recombination represents kinetic behavior ideal for electrical power generation in dye sensitized solar cells.[1] However, when the sensitizers with OPE bridge units were employed with standard $I^-/I_3^-$ redox mediators, the incident photon-to-current efficiencies were poor, less than 0.50. Under the same conditions, **AK0**/$TiO_2$ gave nearly quantitative conversion efficiencies, behavior consistent with this class of *cis*-$Ru(NCS)_2$ type sensitizers.[52] The ∼30% lower excited state injection yield measured for the longest sensitizer certainly contributes to the lower efficiency, but cannot explain the magnitude of the decreased photocurrent. As the electron transfer kinetics were measured under inert electrolyte conditions while the solar cells also contained redox active iodide−iodine mixtures, it was of interest to quantify reactivity under these conditions.

The oxidized sensitizer was found to react with iodide to yield di-iodide, $I_2^{\bullet-}$, as a product. The detailed mechanism by which $I_2^{\bullet-}$ was formed remains unknown at the $TiO_2$ interfaces, but iodine atom and $I_2^{\bullet-}$ intermediates have been proposed.[70,71] Regardless of the I−I bond forming mechanism, $I_2^{\bullet-}$ is unstable with respect to disproportionation chemistry that yields tri-iodide and iodide. Reaction of the injected electrons with $I_3^-$ was quantified and found to be independent of the structure of the sensitizer. Collectively, the data indicated that regeneration and charge recombination to oxidized iodide acceptors were within experimental error the same for all three sensitizers and did not explain the poor energy conversion efficiency measured with the OPE bridged sensitizers. The data do not support the recent suggestion of a possible kinetic advantage to initiating regeneration reactions further from the $TiO_2$ interface, at least in polar $CH_3CN$ solution.[72]

The standard redox mediator solutions of 0.5 M LiI and 0.05 M $I_2$ were utilized in this study. The equilibrium constant for eq 7 has been reported to be $5.6 \times 10^6$ M$^{-1}$ in acetonitrile. Therefore, the equilibrium concentrations of the iodine species present were 0.05 M $I_3^-$, 0.45 M $I^-$ and ∼$10^{-7}$ M $I_2$.[68,69]

$$I^- + I_2 \rightleftharpoons I_3^- \tag{7}$$

Titration of 1 M iodide or tri-iodide into the acetonitrile electrolyte surrounding a sensitized thin film had no measurable influence on the MLCT absorption spectra of the sensitizers. However, the addition of $I_2$ to the external acetonitrile electrolyte surrounding a sensitized thin film resulted in significant spectral changes could be reversed by dilution or by addition of TBAI that decreased the $I_2$ concentration through the equilibrium in eq 7. Taken together, these observation are consistent with the formation of a sensitizer−$I_2$ adduct as was recently reported by O'Regan and co-workers.[73] Adsorption isotherm data revealed an adduct formation constant of about $K = 1.8 \pm 0.2 \times 10^4$ M$^{-1}$ that was in reasonable agreement with their data for similar *cis*-$Ru(NCS)_2$ sensitizers that possess an isothiocyante ligand for $I_2$ coordination.[73]

Pulsed laser excitation of these adducts did not appreciably change the injection yield for **AK0***/$TiO_2$, but decreased the yield by about 80% for the phenylene ethynylene bridged sensitized films. Molecular $I_2$ is an electron acceptor that could reductively quench the excited state to yield the oxidized sensitizer and $I_2^{\bullet-}$, thereby lowering the injection yield.[74,75] While the concentration of $I_2$ is expected to be quite low based on the equilibrium in eq 7, the value might be larger within the sensitized semiconductor mesopores and could account, at least in part, for the low photocurrent efficiencies measured in operational solar cells. Indeed, recent solid state studies indicate that *cis*-$Ru(dcb)_2(NCS)_2$ displays enhanced interactions with $I_2$ relative to $I_3^-$.[76] The data here reveal for the first time an unwanted consequence of remote excited state injection in redox active electrolytes: excited state quenching by redox mediators that lowers the efficiency for electron injection.

The $V_{oc}$ values measured for phenylene ethynylene bridged sensitized $TiO_2$ in the *absence* of redox mediators displayed the largest dependence on irradiance that has been measured. The slopes abstracted from plots of $V_{oc}$ versus the log of the incident irradiance were greater than 180 mV/decade where "ideal" behavior, based on a Schottky junction model of the semiconductor electrolyte interface, is 59 mV/decade. As this


dx.doi.org/10.1021/ja402193f | J. Am. Chem. Soc. 2013, 135, 8331−8341

model is inapplicable to these nanocrystalline thin films, the origin of the open circuit photovoltage has been the subject of many theoretical and experimental studies.[77] One wishes to understand how the quasi-Fermi level of the fluorine doped tin oxide substrate is influenced by the number of electrons present within the $TiO_2$ nanocrystallites. There exists significant experimental and theoretical data that implicate the presence of an exponential distribution of acceptor states in $TiO_2$.[77] The data measured herein support this picture. The chemical capacitance measured experimentally is proportional to the number density of acceptor states per unit energy and reveals that a factor of 10 increase in the injected charge corresponds to a 360 mV increase in voltage. Therefore, ideal behavior at these interfaces is not the 59 mV of an ideal Schottky junction, but 360 mV, and deviations from this must be attributable to charge recombination.

The more rapid charge recombination for $\mathbf{AK0}^+/TiO_2(e^-)$ results in the largest deviation from the expected 360 mV/decade and hence the smallest ideality factor. To fully correlate the $V_{oc}$ dependence on irradiance, one must quantify how charge recombination rates depend on the quasi-Fermi level of the $TiO_2$. Qualitatively, the phenylene ethynylene bridges slow down recombination particularly when the $TiO_2(e^-)$ concentration is large and the quasi-Fermi level is high which would certainly give rise to the more ideal ~180 mV/decade change in $V_{oc}$ measured with these sensitizers. This discussion underscores the importance of measuring ideality factors and charge recombination rate constants over a wide range of irradiances rather than a single $V_{oc}$ value measured under one sun, that is, 100 mW/cm$^2$, as is commonly done.[2]

## CONCLUSION

The photophysical properties of three polypyridyl compounds varying in length, from ~6 to 18.6 Å, that maintain a $Ru(NCS)_2(bpy)$ core with variable number of OPE bridge units were characterized by spectroscopic and electrochemical methods in fluid solution and when anchored to nanocrystalline $TiO_2$ thin films immersed in $CH_3CN$ electrolyte. For the first time, Stark spectroscopy was utilized as an *in situ* probe of the average electric field experienced by sensitizers with variable bridge lengths, and this data was correlated with a distance dependence inferred from electron transfer kinetic measurements. The bridge length dependence for charge recombination was consistent with the attenuation factor of $\beta$ = 0.12 Å$^{-1}$. Inhibited $S^+/TiO_2(e^-) \rightarrow S/TiO_2$ charge recombination is beneficial for solar energy conversion as larger steady state concentrations of injected electrons can be realized. Slow recombination is important in regenerative dye sensitized solar cells when $S^+$ is a weak oxidant as well as for photoelectrosynthetic water splitting cells where the rates of water oxidation are generally small. Furthermore, the strong irradiance dependence of the recombination rate constants and $V_{oc}$ values reveal the dangers of comparative studies measured only at one irradiance and surface coverage. Finally, an unwanted consequence of excited state injection from sensitizers with long bridge units was identified, excited state quenching by redox mediators present in the electrolyte, that can possibly be avoided in the future through judicious choice of the redox mediator.

## ASSOCIATED CONTENT

### Supporting Information

Physical methods, spectroscopic, and electrochemical data, as well as videos of the charge recombination data as the $TiO_2(e^-)$ concentration was increased with an external bias. This material is available free of charge via the Internet at http://pubs.acs.org.

## AUTHOR INFORMATION

### Corresponding Author

meyer@jhu.edu; galoppin@andromeda.rutgers.edu

### Notes

The authors declare no competing financial interest.

## ACKNOWLEDGMENTS

This work was funded by the Division of Chemical Sciences, Geosciences, and Biosciences, Office of Basic Energy Sciences of the U.S. Department of Energy through Grant DE-FG02-01ER15256 (E.G.) and Grant DE-FG02-96ER14662 (G.J.M.). The authors would also like to thank Professor Doug Barrick and Jake Marold for use of the Model 14NT-UV−vis Aviv spectrophotometer.

## REFERENCES

(1) Ardo, S.; Meyer, G. J. *Chem. Soc. Rev.* **2009**, *38*, 115−164.
(2) Hagfeldt, A.; Gratzel, M. *Acc. Chem. Res.* **2000**, *33*, 269−277.
(3) Yella, A.; Lee, H.-W.; Tsao, H. N.; Yi, C.; Chandiran, A. K.; Nazeeruddin, M. K.; Diau, E. W.-G.; Yeh, C.-Y.; Zakeeruddin, S. M.; Gratzel, M. *Science* **2011**, *334*, 629−634.
(4) O'Regan, B.; Gratzel, M. *Nature* **1991**, *353*, 737−740.
(5) O'Regan, B. C.; Durrant, J. R. *Acc. Chem. Res.* **2009**, *42*, 1799−1808.
(6) Benko, G.; Kallioinen, J.; Korppi-Tommola, J. E. I.; Yartsev, A. P.; Sundstrom, V. *J. Am. Chem. Soc.* **2001**, *124*, 489−493.
(7) Asbury, J. B.; Ellingson, R. J.; Ghosh, H. N.; Ferrere, S.; Nozik, A. J.; Lian, T. *J. Phys. Chem. B* **1999**, *103*, 3110−3119.
(8) Monat, J. E.; McCusker, J. K. *J. Am. Chem. Soc.* **2000**, *122*, 4092−4097.
(9) Hannappel, T.; Burfeindt, B.; Storck, W.; Willig, F. *J. Phys. Chem. B* **1997**, *101*, 6799−6802.
(10) Tachibana, Y.; Moser, J. E.; Gratzel, M.; Klug, D. R.; Durrant, J. R. *J. Phys. Chem.* **1996**, *100*, 20056−20062.
(11) Benko, G.; Kallioinen, J.; Korppi-Tommola, J. E. I.; Yartsev, A. P.; Sundstrom, V. *J. Am. Chem. Soc.* **2002**, *124*, 489−493.
(12) Farzad, F.; Thompson, D. W.; Kelly, C. A.; Meyer, G. J. *J. Am. Chem. Soc.* **1999**, *121*, 5577−5578.
(13) Higgins, G. T.; Bergeron, B. V.; Hasselmann, G. M.; Farzad, F.; Meyer, G. J. *J. Phys. Chem. B* **2006**, *110*, 2598−2605.
(14) Altobello, S.; Argazzi, R.; Caramori, S.; Contado, C.; Da Fre, S.; Rubino, P.; Chone, C.; Larramona, G.; Bignozzi, C. A. *J. Am. Chem. Soc.* **2005**, *127*, 15342−15343.
(15) Smalley, J. F.; Sachs, S. B.; Chidsey, C. E. D.; Dudek, S. P.; Sikes, H. D.; Creager, S. E.; Yu, C. J.; Feldberg, S. W.; Newton, M. D. *J. Am. Chem. Soc.* **2004**, *126*, 14620−14630.
(16) Pettersson, K.; Kyrychenko, A.; Ronnow, E.; Ljungdahl, T.; Martensson, J.; Albinsson, B. *J. Phys. Chem. A* **2005**, *110*, 310−318.
(17) Scott, A. M.; Wasielewski, M. R. *J. Am. Chem. Soc.* **2011**, *133*, 3005−3013.
(18) Heimer, T. A.; D'Arcangelis, S. T.; Farzad, F.; Stipkala, J. M.; Meyer, G. J. *Inorg. Chem.* **1996**, *35*, 5319−5324.
(19) Neale, N. R.; Kopidakis, N.; van de Lagemaat, J.; Gratzel, M.; Frank, A. J. J. *Phys. Chem. B* **2005**, *109*, 23183−23189.
(20) Trammell, S. A.; Meyer, T. J. J. *Phys. Chem. B* **1998**, *103*, 104−107.
(21) Bergeron, B. V.; Kelly, C. A.; Meyer, G. J. *Langmuir* **2003**, *19*, 8389−8394.

(22) Zaban, A.; Chen, S. G.; Chappel, S.; Gregg, B. A. *Chem. Commun.* **2000**, 2231−2232.
(23) Palomares, E.; Clifford, J. N.; Haque, S. A.; Lutz, T.; Durrant, J. R. *J. Am. Chem. Soc.* **2003**, *125*, 475−482.
(24) Clifford, J. N.; Palomares, E.; Nazeeruddin, M. K.; Gratzel, M.; Nelson, J.; Li, X.; Long, N. J.; Durrant, J. R. *J. Am. Chem. Soc.* **2004**, *126*, 5225−5233.
(25) Argazzi, R.; Bignozzi, C. A.; Heimer, T. A.; Castellano, F. N.; Meyer, G. J. *J. Am. Chem. Soc.* **1995**, *117*, 11815−11816.
(26) Bonhote, P.; Moser, J.; Humphry-Baker, R.; Vlachopoulos, N.; Zakeeruddin, S. M.; Walder, L.; Gratzel, M. *J. Am. Chem. Soc.* **1999**, *121*, 1324−1336.
(27) Haque, S. A.; Handa, S.; Peter, K.; Palomares, E.; Thelakkat, M.; Durrant, J. R. *Angew. Chem., Int. Ed.* **2005**, *44*, 5740−5744.
(28) Hu, K.; Robson, K. C. D.; Johansson, P. G.; Berlinguette, C. P.; Meyer, G. J. *J. Am. Chem. Soc.* **2012**, *134*, 8352−8354.
(29) Abrahamsson, M.; Johansson, P. G.; Ardo, S.; Kopecky, A.; Galoppini, E.; Meyer, G. J. *J. Phys. Chem. Lett.* **2011**, *1*, 1725−1728.
(30) Bublitz, G. U.; Boxer, S. G. *Annu. Rev. Phys. Chem.* **1997**, *48*, 213−242.
(31) Wang, P.; Zakeeruddin, S. M.; Moser, J. E.; Nazeeruddin, M. K.; Sekiguchi, T.; Gratzel, M. *Nat. Mater.* **2003**, *2*, 402−407.
(32) Grosshenny, V.; Romero, F. M.; Ziessel, R. *J. Org. Chem.* **1997**, *62*, 1491−1500.
(33) Hofmeier, H.; El-ghayoury, A.; Schenning, A. P. H. J.; Schubert, U. S. *Tetrahedron* **2004**, *60*, 6121−6128.
(34) Rajesh, K.; Somasundaram, M.; Saiganesh, R.; Balasubramanian, K. K. *J. Org. Chem.* **2007**, *72*, 5867−5869.
(35) Lee, C.-H.; Galoppini, E. *J. Org. Chem.* **2010**, *75*, 3692−3704.
(36) Sprecher, M.; Breslow, R.; Uziel, O.; Link, T. M. *Org. Prep. Proced. Int.* **1994**, *26*, 696−701.
(37) Jang, S.-R.; Yum, J.-H.; Klein, C.; Kim, K.-J.; Wagner, P.; Officer, D.; Gratzel, M.; Nazeeruddin, M. K. *J. Phys. Chem. C* **2009**, *113*, 1998−2003.
(38) Klein, C.; Nazeeruddin, M. K.; Liska, P.; Di Censo, D.; Hirata, N.; Palomares, E.; Durrant, J. R.; Gratzel, M. *Inorg. Chem.* **2004**, *44*, 178−180.
(39) Theodorou, V.; Skobridis, K.; Tzakos, A. G.; Ragoussis, V. *Tetrahedron Lett.* **2007**, *48*, 8230−8233.
(40) Nazeeruddin, M. K.; Zakeeruddin, S. M.; Humphry-Baker, R.; Jirousek, M.; Liska, P.; Vlachopoulos, N.; Shklover, V.; Fischer, C.-H.; Gratzel, M. *Inorg. Chem.* **1999**, *38*, 6298−6305.
(41) Chen, Z.; Concepcion, J. J.; Luo, H.; Hull, J. F.; Paul, A.; Meyer, T. J. *J. Am. Chem. Soc.* **2011**, *132*, 17670−17673.
(42) Pavlishchuk, V. V.; Addison, A. W. *Inorg. Chim. Acta* **2000**, *298*, 97−102.
(43) Morris, A. J.; Marton, A.; Meyer, G. J. *Inorg. Chem.* **2008**, *47*, 7681−7685.
(44) De Angelis, F.; Fantacci, S.; Selloni, A.; Nazeeruddin, M. K. *Chem. Phys. Lett.* **2005**, *415*, 115−120.
(45) Wang, D.; Mendelsohn, R.; Galoppini, E.; Hoertz, P. G.; Carlisle, R. A.; Meyer, G. J. *J. Phys. Chem. B* **2004**, *108*, 16642−16653.
(46) Morris, A. J.; Meyer, G. J. *J. Phys. Chem. C* **2008**, *112*, 18224−18231.
(47) Ondersma, J., W.; Hamann, T. W. *Energy Environ. Sci.* **2012**, *5*, 9476−9480.
(48) Fabregat-Santiago, F.; Mora-Sero, I.; Garcia-Belmonte, G.; Bisquert, J. *J. Phys. Chem. B* **2002**, *107*, 758−768.
(49) Langmuir, I. *J. Am. Chem. Soc.* **1918**, *40*, 1361−1403.
(50) Williams, G.; Watts, D. C. *Trans. Faraday. Soc* **1970**, *66*, 80−85.
(51) Rowley, J. G.; Meyer, G. J. *J. Phys. Chem. C* **2011**, *115*, 6156−6161.
(52) Nazeeruddin, M. K.; Kay, A.; Rodicio, R.; Humphry-Baker, R.; Muller, P.; Liska, P.; Vlachopoulos, N.; Gratzel, M. *J. Am. Chem. Soc.* **1993**, *115*, 6382−6390.
(53) Qu, P.; Meyer, G. J. *Langmuir* **2001**, *17*, 6720−6728.
(54) Ardo, S.; Sun, Y.; Staniszewski, A.; Castellano, F. N.; Meyer, G. J. *J. Am. Chem. Soc.* **2011**, *132*, 6696−6709.
(55) Boxer, S. G. *J. Phys. Chem. B* **2009**, *113*, 2972−2983.
(56) Waterland, M. R.; Kelley, D. F. *J. Phys. Chem. A.* **2001**, *105*, 4019−4028.
(57) Zaban, A.; Ferrere, S.; Gregg, B. A. *J. Phys. Chem. B* **1998**, *102*, 452−460.
(58) Katoh, R.; Furube, A. *J. Phys. Chem. Lett.* **2011**, *2*, 1888−1891.
(59) O'Regan, B.; Moser, J.; Anderson, M.; Graetzel, M. *J. Phys. Chem.* **1990**, *94*, 8720−8726.
(60) Haque, S. A.; Tachibana, Y.; Klug, D. R.; Durrant, J. R. *J. Phys. Chem. B* **1998**, *102*, 1745−1749.
(61) Nelson, J. *Phys. Rev. B* **1999**, *59*, 15374−15380.
(62) Cao, F.; Oskam, G.; Meyer, G. J.; Searson, P. C. *J. Phys. Chem.* **1996**, *100*, 17021−17027.
(63) Huang, S. Y.; Schlichthorl, G.; Nozik, A. J.; Gratzel, M.; Frank, A. J. *J. Phys. Chem. B* **1997**, *101*, 2576−2582.
(64) Peter, L. M.; Duffy, N. W.; Wang, R. L.; Wijayantha, K. G. U. *J. Electroanal. Chem.* **2002**, *524*−*525*, 127−136.
(65) Vargas-Florencia, D.; Edvinsson, T.; Hagfeldt, A.; Furo, I. *J. Phys. Chem. C* **2007**, *111*, 7605−7611.
(66) Kuciauskas, D.; Freund, M. S.; Gray, H. B.; Winkler, J. R.; Lewis, N. S. *J. Phys. Chem. B* **2000**, *105*, 392−403.
(67) Hasselmann, G. M.; Meyer, G. J. *J. Phys. Chem. B* **1999**, *103*, 7671−7675.
(68) Boschloo, G.; Hagfeldt, A. *Acc. Chem. Res.* **2009**, *42*, 1819−1826.
(69) Rowley, J. G.; Farnum, B. H.; Ardo, S.; Meyer, G. J. *J. Phys. Chem. Lett.* **2011**, *1*, 3132−3140.
(70) Gardner, J. M.; Abrahamsson, M.; Farnum, B. H.; Meyer, G. J. *J. Am. Chem. Soc.* **2009**, *131*, 16206−16214.
(71) Clark, C. C.; Marton, A.; Srinivasan, R.; Narducci Sarjeant, A. A.; Meyer, G. J. *Inorg. Chem.* **2006**, *45*, 4728−4734.
(72) Clark, C. C.; Meyer, G. J.; Wei, Q.; Galoppini, E. *J. Phys. Chem. B* **2006**, *110*, 11044−11046.
(73) Li, X.; Reynal, A.; Barnes, P. R. F.; Humphry-Baker, R.; Zakeeruddin, S. M.; De Angelis, F.; O'Regan, B. C. *Phys. Chem. Chem. Phys.* **2012**, *14*, 15421−15428.
(74) Stanbury, D. M.; Sykes, A. G. In *Advances in Inorganic Chemistry*; Academic Press: San Diego, 1989; Vol. 33, pp 69−138.
(75) Wilmarth, W. K.; Stanbury, D. M.; Byrd, J. E.; Po, H. N.; Chua, C.-P. *Coord. Chem. Rev.* **1983**, *51*, 155−179.
(76) Tuikka, M.; Hirva, P.; Rissanen, K.; Korppi-Tommola, J.; Haukka, M. *Chem. Commun.* **2011**, *47*, 4499−4501.
(77) Bisquert, J.; Fabregat-Santiago, F.; Mora-Sera, I. n.; Garcia-Belmonte, G.; Barea, E. M.; Palomares, E. *Inorg. Chim. Acta* **2008**, *361*, 684−698.